Volume 13, Number 2, 2020. pp. 171-179

Jordan Journal of Physics

ARTICLE

Similarities and Differences between Two Researches in Field Electron Emission: A Way to Develop a More Powerful Electron Source

M. S. Mousa[a], **A. Knápek**[b] and **L. Grmela**[c]

[a] *Department of Physics, Mu'tah University, Al-Karak 61710, Jordan.*
[b] *Institute of Scientific Instruments of the CAS, Královopolská 147, Brno 61264, Czech Republic.*
[c] *Department of Physics, Brno University of Technology, Technická 8, Brno 61600, Czech Republic.*

Doi : https://doi.org/10.47011/13.2.9

Received on: 28/11/2019; *Accepted on: 20/2/2020*

Abstract: This paper discusses the similarities and differences between two studies that deal with resin-coated field-emission cathodes. The two works that are compared within this paper are entitled: *Hot Electron Emission from Composite-Insulator Micropoint Cathodes* and *Methods of Preparation and Characterization of Experimental Field-Emission Cathodes*. Within the text, both studies are reviewed and put into context, pointing out and commenting the advantageous features of this type of cathodes. The comparison focuses mainly on the method of preparation including deposition of a thin film on the cathode tip and the characterization of the coating itself. The effect of the coating on the field emission is discussed as well.
Keywords: Cold field emission, Epoxylite 478, Epoxylite EPR-4.

Introduction

At present, field electron emission from a metal through a dielectric layer is a subject of considerable interest. Its importance is caused mainly by electron devices utilizing a focused electron beam which requires a high-quality source of free electrons that is sufficiently bright and able to provide high current density and work in low-quality vacuum conditions [1, 2]. This paper discusses and further compares two experimental emitters appearing in two separate projects, implying a single way to develop the ultimate electron source.

An experimental field-emission emitter based on tungsten ultra-sharp emitter with a metal-oxide-dielectric structure proved to be the ideal candidate based on the conditions stated above. Regarding the advantages of cold field-emission sources, it should be emphasized that only slight demagnification is required to obtain a 1nm-diameter probe, because of the small virtual source starting from 2 up to 5 nm [2]. Secondly, there is only a very small energy spread, which enables operation at low accelerating voltages. This, in turn, enables to obtain a very sharp, high-contrast image without major radiation damage, especially when working with biological specimens (e.g. tissues or single cells). Lastly, thanks the epoxy layer, it is possible to work in relatively low-quality vacuum (less than 10^{-6} Pa), preventing the ion-bombardment and chemi/physisorption of residuals on the surface of the tip. The preservation of the lower vacuum also enables faster manipulation with the sample and a generally lower price compared to devices working with UHV exceeding 10^{-7} Pa [2].

Corresponding Author: Marwan. S. Mousa **Email**: mmousa@mutah.edu.jo

The need for a better understanding of high-voltage phenomena and development of theories of field electric emission from epoxy-coated tips represents the motivation to study further the behavior of composite tips [1-4]. In general, field electron emission occurs after switch-on voltage is applied to the tip, which has been introduced in previous papers [5-8]. This produces an emission current at considerably lower voltage compared to pure (virgin) tungsten cathodes. Cycling of the voltage provides reproducible I-V characteristics [7,8] with an improved stability [9,10] and a brighter spot [11].

The summary that is presented in this paper concerns our investigations carried out under high vacuum following the pressure 10^{-6} Pa and baking the system at 150–200 °C. In this work, all the experiments were carried out using a high-purity single/polycrystalline tungsten wire, due to its favorable properties, such as: high melting point, high hardness, high work function and significant heat resistance at high temperatures [1-4].

Methods of Preparing Cathodes

Ultra-sharp tips used as a metallic substrate of epoxy-coated emitters were prepared by the same method based on electrolytic etching in both cases [1, 2]. For the electrolyte, a solution of 2–2.5 molar sodium hydroxide was used. After applying the two-phase etching method [4], the samples were cleaned by HF and ethylene (or isopropyl alcohol) in the first step. In the second step, the samples were further cleaned in water for a few minutes using ultrasonic bath in order to get rid of the contaminants originating from the electrochemical etching that are discussed further in the text. The composition of a typical cathode is obtained by Energy Dispersive X-ray spectroscopy (EDS), as illustrated in Fig. 1.

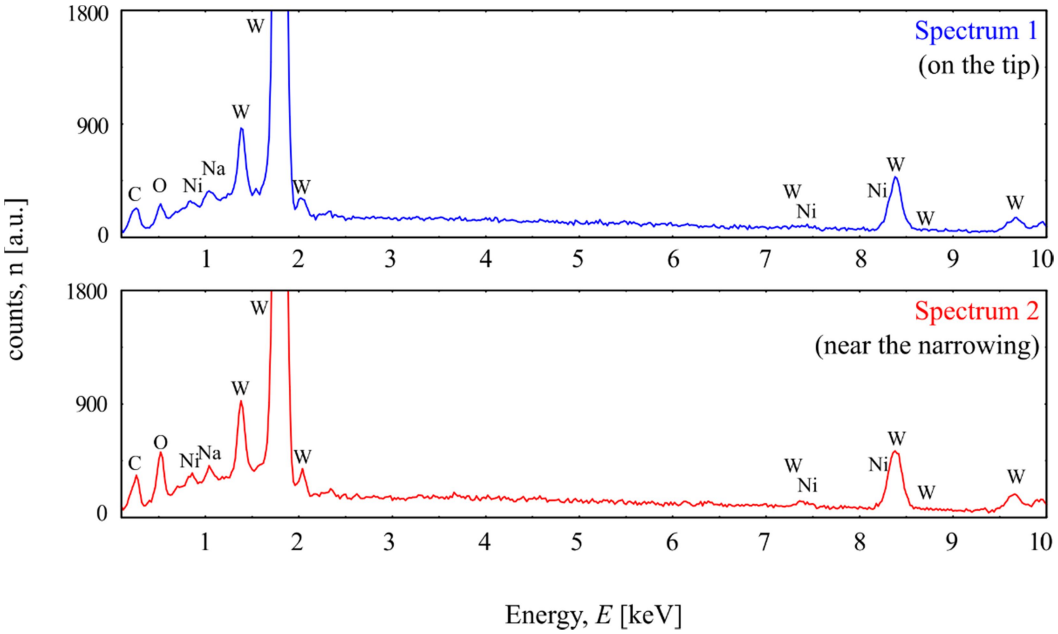

FIG. 1. The spectra of the SEM-EDS analysis for a sample coated by (*478 Epoxy resin*) a) EDS on the tip (blue). b) EDS in the area of wire narrowing (red).

From the results of the EDS analysis of the second emitter, it can be seen that even though tungsten predominates, there is a certain amount of contaminants present. The EDS spectrum was measured twice: on the coated surface (blue) and on the narrowing (uncoated area). Both measurements are comparable and show only a limited influence of the epoxy thin film on the chemical composition. Contaminants, such as Nickel (Ni) and Sodium (Na), originate from a grounded electrode (cathode) that releases some of the components from its surface during the etching process.

These contaminants move from the cathode towards the etched tip and attach to the surface of the etched tip. Despite the fact that this analysis was performed only in the second study, it can be concluded that it goes also for the first study, since it depends on the chemical composition of the etched wire (that was pure

tungsten in both cases) and on the composition of the grounded electrode (that was steel in both cases as well).

After the final etching step, the tip was in both cases coated by epoxy resin: in the first paper, commercially available resin branded *Epoxylite UPR-4* is used, whereas in the second paper, the *Epoxylite 478* is used. In both cases, resins are cured in an electric furnace at two different phases, each at a different temperature. The first phase, where the temperature is usually about 100 °C, serves for degassing of the epoxy. The second phase serves for reaching the glass transition temperature. Fig. 2 shows the emitters coated by using transmission electron microscopy (TEM) and scanning electron microscopy (SEM). The TEM shows a slight difference of the contrast between the dielectric layer and the metallic core. The SEM, on the other hand, shows surface contrast and hence the part of the tip that has been coated. Both methods are complementary and provide different information about coating. The coating method itself in both cases is based on dipping the tip in the epoxy and covering the very top of the tip by a homogeneous layer.

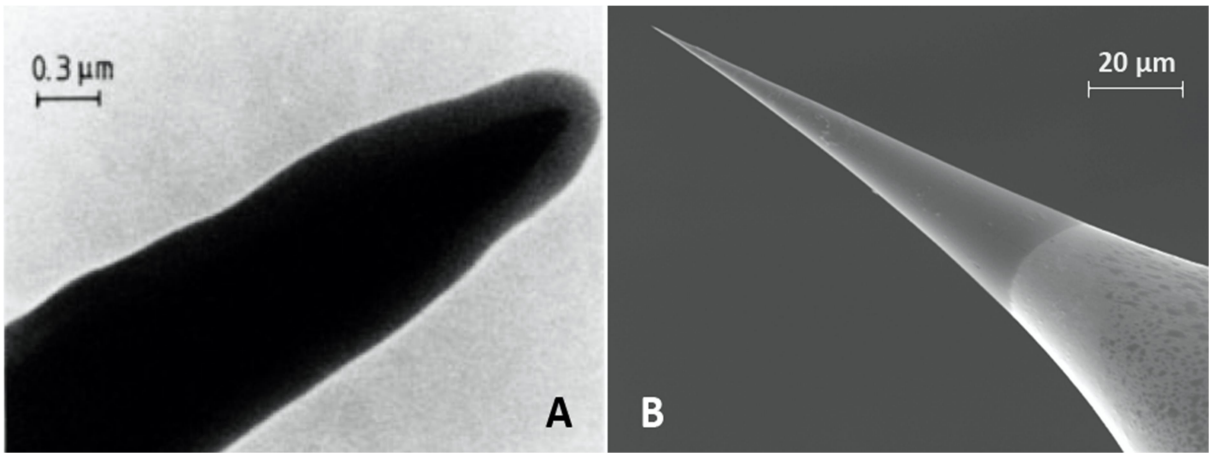

FIG. 2. a) TEM micrograph of W-tip coated by *Epoxylite UPR-4* with a diameter of approx. 200 nm; b) SEM micrograph of W-tip coated by *Epoxylite 478* with a diameter of approx. 20–30 nm.

In the first case, the tip is dipped twelve times into the Epoxylite UPR-4 epoxy, where the concentration ratio of the A and B components was 1:1. The single dip creates a layer that is approximately 15 nm thick. The ultra-sharp tips used as a metallic substrate of the epoxy-coated emitters were prepared by using the same method based on electrolytic etching in both cases [1, 2]. The layer thickness is approximately 200 nm. In the second case, the tip is dipped only once into the Epoxylite 478 which is a single component epoxy resin creating a layer of 20–30nm thickness. Both epoxy resins are based on a *Bisphenol A diglycidyl ether* which is a colorless solid that melts slightly above room temperature. The UPR-4 is a two-component epoxy, whilst the 478 is a single-component epoxy. The difference in thickness amongst the two epoxy resins is caused mainly by different densities of the epoxy resins. In both cases, the tip is then subjected to a curing cycle. In the first case, the tip is baked directly in the vacuum chamber during the degassing procedure, whilst in the second case, the tip is cured in the electric oven. The first part of the curing procedure takes thirty minutes at 100 °C to expel the solvents, followed by thirty minutes at 160 °C to complete the curing of the resin [2, 3]. In both cases, the epoxy resin undergoes glass transition and becomes a hard and relatively brittle “glassy” matter.

Comparison of the Experimental Results

In this part, the experimental results obtained by several methods are described and compared in more detail. Those methods are, in particular:

a) Current-voltage (I-V) characterization and Fowler-Nordheim (F-N) analysis of the I-V data,

b) Analysis of the switch-on phenomena and the emission patterns,

c) Energy and noise spectral analysis of the electron beam.

a. Current-Voltage Characterization and Fowler-Nordheim Analysis

The I-V curve is used to determine basic parameters of the field-emission cathode and to model its behavior during operation. In Fig. 3, curve A shows the I-V characteristics for an uncoated tungsten emitter with a 30nm tip apex connected in a simple diode configuration. Compared to curve A, curve B represents the characteristics of a coated tip by 200 nm of Epoxylite UPR-4 resin. It can be seen that the threshold voltage V_{th} decreased and an additional hysteresis appeared, slightly moving the characteristics toward higher current values when the applied voltage is increased in contrary to the opposite way. These effects have been already described and discussed in several papers [1, 5, 7].

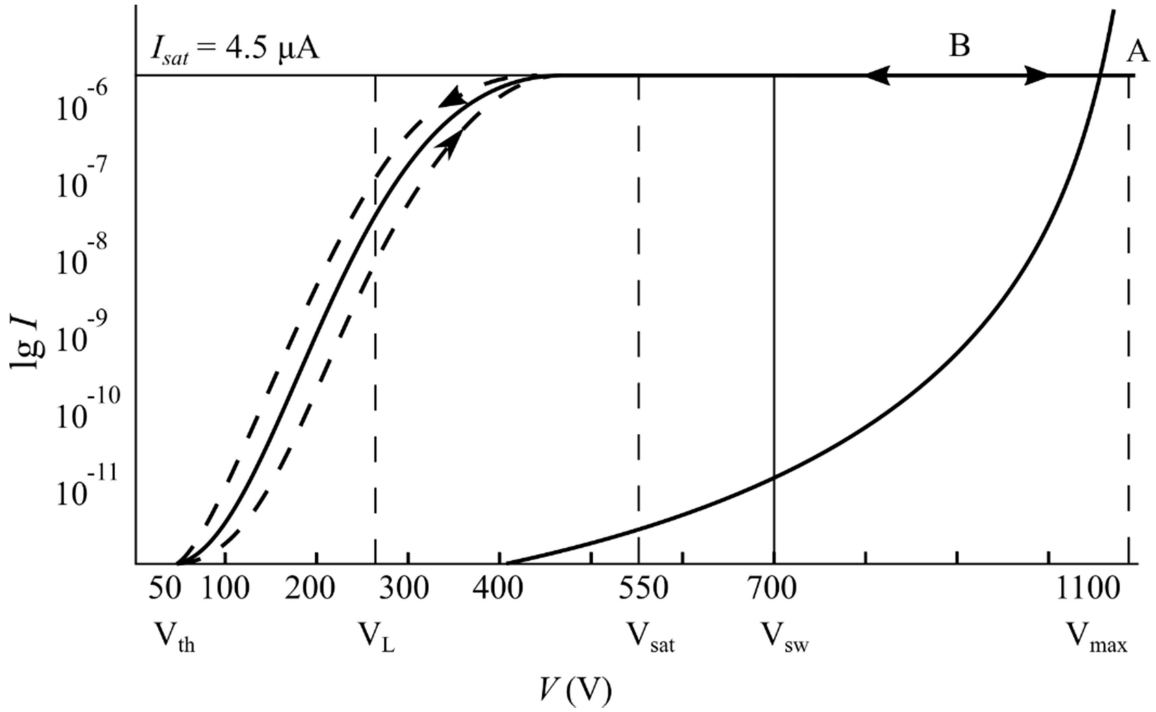

FIG. 3. A comparison of I-V characteristics of an uncoated (A) *vs.* coated (B) W-emitter of a tip radius of 30 nm and an epoxy coating of approx. 200 nm (*UPR-4 Epoxylite resin*).

Fig.4 shows the Fowler-Nordheim plots of the uncoated (curve A) and the resin-coated (Epoxylite UPR-4) sharp tip. The Fowler-Nordheim plot is the most common method of analyzing the I-V characteristics and it is used to graphically interpret and analyze data obtained from the theoretical equation derived by Fowler-Nordheim [11]. The original idea was to obtain an exact straight line of slope S_{FN}, which would be a ratio related to the parameters appearing in the exponent of a Fowler-Nordheim-type equation of I-V form by: $S_{FN} = -b\varphi^{3/2}/\beta$; and therefore the knowledge of the work-function φ would enable the determination of field enhancement factor β and *vice versa*. From Fig. 4, a certain difference between slopes of lines representing uncoated (A) and coated (B) emitters can be seen. A decrease in the slope of the F-N plots of the coated cathode at room temperature is obtained with a factor β of 3 to 4. This also results in a decrease in the work function φ with respect to that of the uncoated W-tip of 4.52 eV [5].

In Fig. 5, the left curve shows the I-V characteristic for a sample coated with (478 Epoxylite resin) [4, 8]. The cathode was measured in the triode mode incorporating an additional anode called *the extractor* electrode which is located close (approx. 0.75 mm) to the field emission tip. This configuration is used mostly for devices utilizing a focused electron beam, where it is possible to change the size of the cross-over simply by changing the ratio between voltages applied. The extractor electrode makes the electrons leave the surface and the additional (acceleration) energy is provided by the anode which serves as the main acceleration electrode here. The particular set-up and the precise measurement method is described in more detail by Knápek [4].

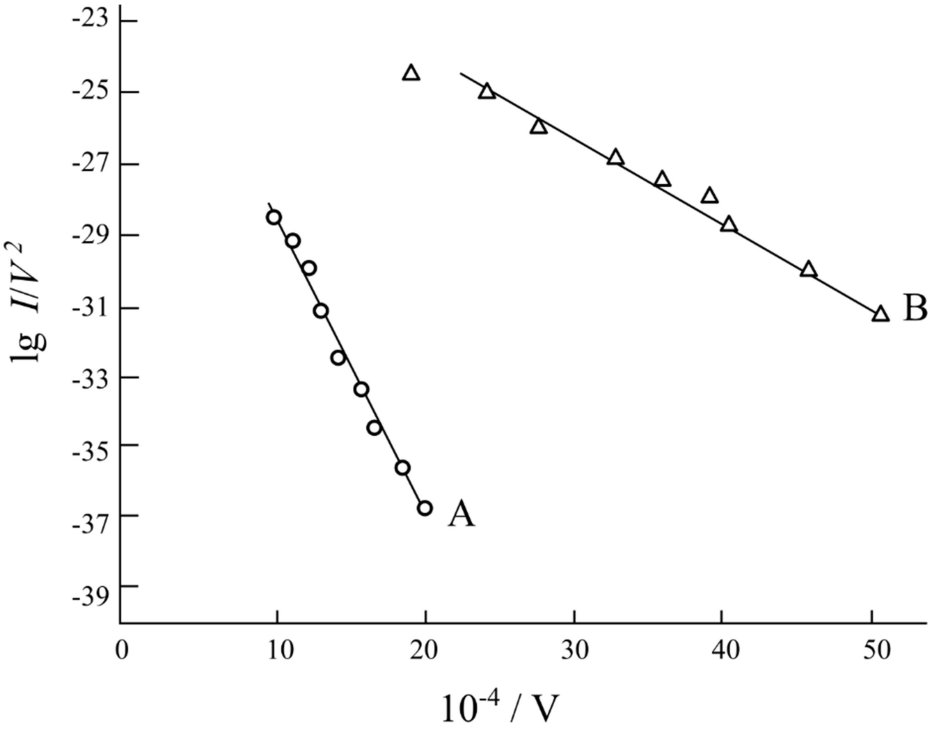

FIG. 4. The Fowler-Nordheim plots of the uncoated (curve A) and *Epoxylite UPR-4* coated tip (curve B).

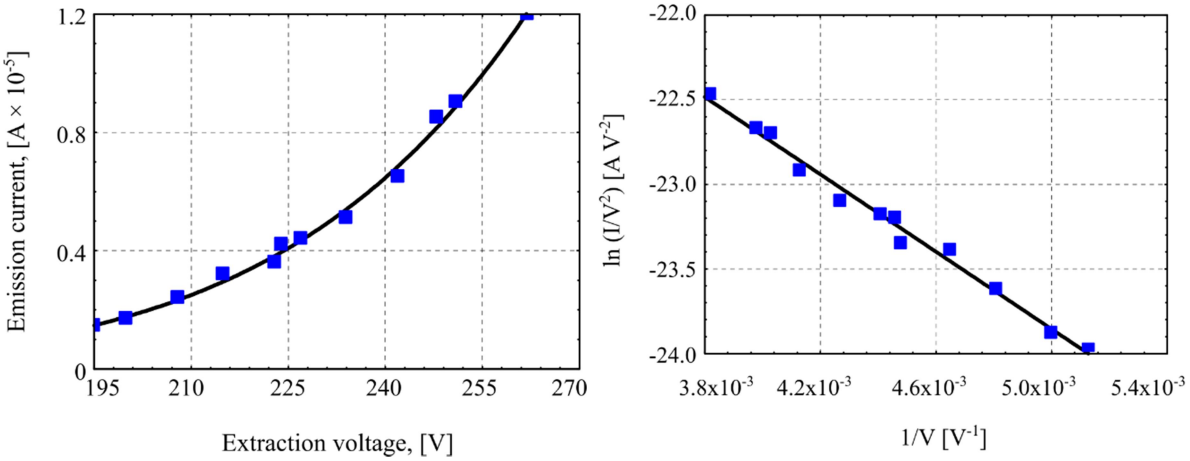

FIG. 5. Electrical characteristics of the tip coated by *Epoxylite 478*. Left: I-V characteristics of the emission current based on extraction voltage following exponential function. Right: calculated Fowler-Nordheim plot following linear slope.

The current-voltage measurements of the second sample are represented by Fig. 5 left (I-V characteristics) and right (F-N plot). Even though the I-V characteristics curve covers just a limited range of extraction voltages (195–270 V), it implies that the current there follows the same exponential function as the previous coated sample illustrated in Fig. 3. B. The difference of the nominal current is caused mainly by a different operation mode (the triode mode *vs*. the diode mode), by a different detection method (the Al-coated scintillation crystal *vs*. phosphorus screen in the previous case) and by different coating where both layer thickness and different chemical structure affect the emission. In the F-N plot illustrated in the right part of Fig. 5, it can be seen that there is a certain similarity to the previous sample implying the same effect on the field emission. This effect was explained in more detail by Mousa [12].

The ideal thickness of the Epoxylite 478 coating whose relative permittivity $\varepsilon_r = 4$ has been theoretically calculated (based on WKB approximation) and found to be around 5 nm [2].

To conclude this part, the typical slope of a coated emitter is ≈ 1/4 that of the uncoated tungsten emitter. The maximum voltage that may be applied for stable emission is typically twice the voltage required for saturated emission [1, 6, 8].

b. Analysis of Switch-on Phenomena and Emission Patterns

The initiation of the field emission is observed after a "switch-on" voltage has been applied to the tip. This produces a saturated emission current that can then be maintained at much lower voltages. A summary of the most important results was reviewed in a paper published by Mousa [5]. The projection images that appear on the screen are also referred to as emission patterns due to their geometric arrangement for single-crystalline emitters. In each of the studies, the analysis of the emission pattern is made from a different point of view. For the first paper, the difference between virgin (uncoated) and coated emitters is analyzed, whilst for the second, the effect of the extractor voltage is analyzed for the coated emitter.

The field emission pattern displays the projected work function map of the emitter surface. The closely packed faces {110}, {100}, and {211} have higher work functions than atomically rough regions and they thus appear in the image as dark spots on the brighter background (see Fig. 6. A). In the right part of the figure, the effect of epoxy coating can be seen creating a single emission region in the position of the facet {110}. This is one of the most important and interesting features of using the epoxy coating.

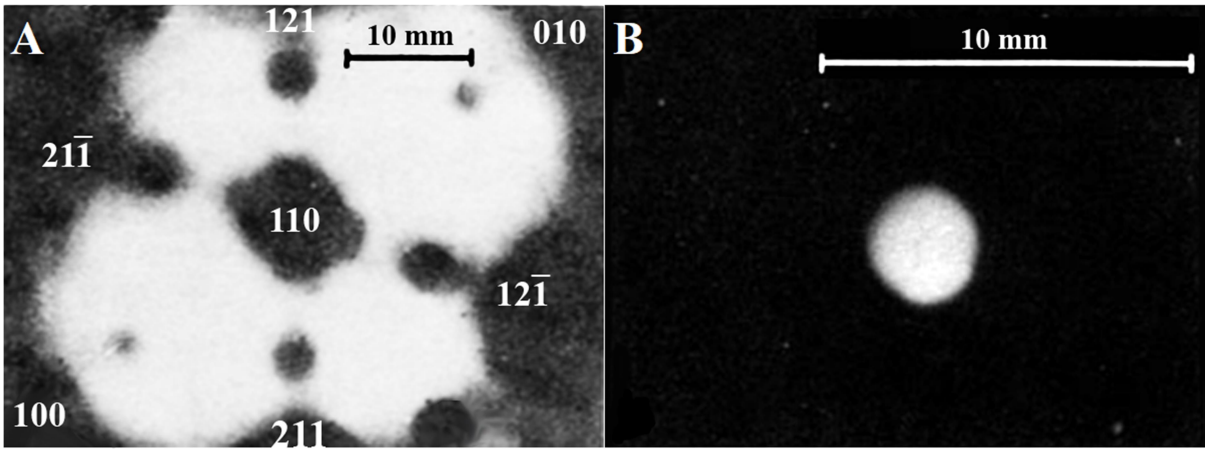

FIG. 6. Emission pattern obtained from a) the clean tungsten emitter and from b) the emitter that was coated by a 150nm layer of *Epoxylite UPR-4* resin. Both images were recorded with the same tip-to-screen separation and the same emission current of 4.5 pA [1, 6].

For the tips that were coated by Epoxylite 478 in the second work, it has been experimented with an increasing extractor voltage and its effect on the shape of the field-emission-active area. Instead of the phosphorus screen used in the previous case, in this case, a Cerium-doped Yttrium Aluminium garnet was used to display the emission pattern and to conduct a constant part of the electron beam that has been used for analysis. The measurement is illustrated in Fig. 7, showing 4 extracting V_{ex} voltages and the corresponding spot size d. It has been found out that the intensity of the spot size is equally distributed and the shape is equidistant in respect to the optical axis. Another pursued parameter is the relative light intensity that is a parameter based on the number of photons impinging on the surface of the CCD chip of a camera used to record the image, which is expressed in percents. Authors have found out that the relative light intensity L follows the linear function [2].

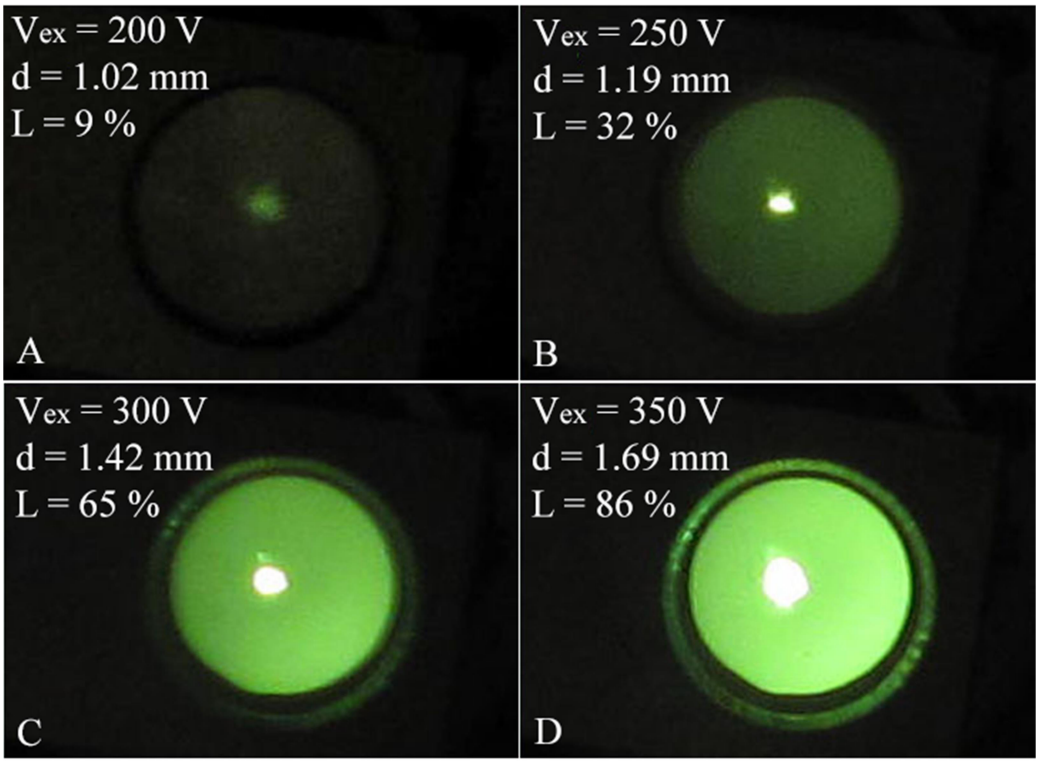

FIG. 7. The emission patterns *vs*. the extraction voltage for the sample coated by *Epoxylite 478* resin [8].

c. Energy and Noise Spectral Analysis of the Electron Beam

The electron spectra were measured only for the cathodes coated by Epoxylite UPR-4 to provide important information on the emission mechanism associated with the composite regimes. The measurements were performed using a well-known retarding potential analyzer design of Van Oostrom (1966), but incorporating fully automated electronically controlled drive and detection systems [1]. In particular, a lock-in amplifier technique was used to obtain a direct differential spectral output providing an output that is comparable to the more widely used hemispherical type of analyzer [1].

Fig. 8 illustrates and compares the energy spectra obtained from a tungsten emitter before (A) and after (B) coating with a 200nm thick layer of the Epoxylite UPR-4 resin. In both cases, the emission currents were equal to 4 pA.

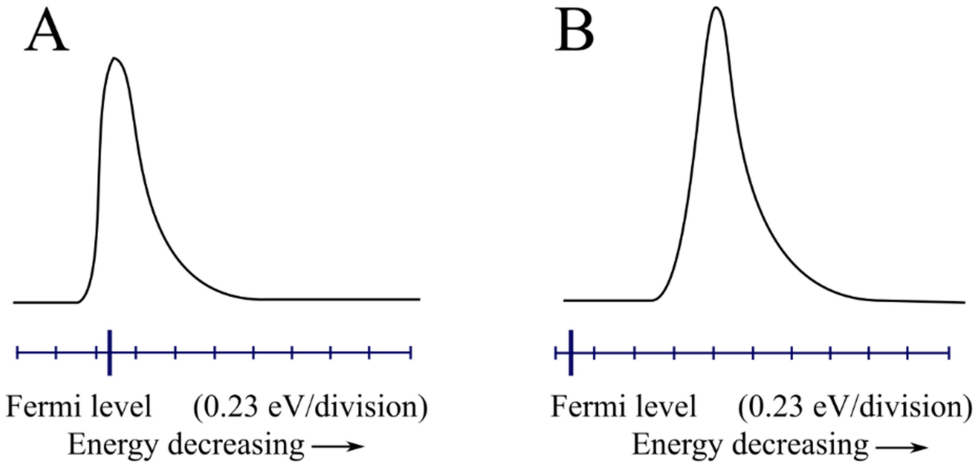

FIG. 8. A comparison of the energy spectra obtained from the tungsten emitter (a) before and (b) after coating with a 150 nm thick layer of resin at identical emission currents of 4 pA.

These results have shown that with respect to the Fermi level, the spectrum obtained in the metal cathode is displaced towards lower energies by approx. 0.7 eV and that the composite emitter has a significantly larger full width at half-maximum compared to the uncoated one. Last, but not least, the measurements showed that the spectrum of the composite emitter is more symmetrical compared to the clean tungsten tip [1, 5].

In the second case, for the Epoxylite 478-coated tip, the electron beam was analyzed using a method that is based on evaluating the slope of the power noise spectral density spectrum of the total emission current. This method is mostly used for semiconductor analysis and it is obtained by performing the Fourier transformation on the sampled emission current. From the slope of the spectrum at particular frequency bands, it is possible to identify processes responsible for particular events that are responsible for the noise at the quantum level. The precise method was described by Knápek [10].

From the measurements shown in Fig. 9, it is evident that the power spectral density of whole spectra is being slowly increased in time and that the slope is staying constant. From the slope, which is constantly about 1.5, it is evident that the measured noise has characteristics of the so-called $1/f$ (flickering) noise. The $1/f$ noise is a process with a frequency spectrum, such that the power spectral density is proportional to the reciprocal of the frequency. We can see that, for the red curve, the parameters changed to $a = 1.5\times10^{-4}$, the slope $n = -1.3$ and the time constant remains the same, $b = 1\times10^{-3}$ s. In conclusion, the period τ between each hop to the different energy level is computed as 1.59×10^{-4} s. The cutting frequency is located near 1000 Hz. The $1/f^{n}$ noise (where $n > 1$) originates from the superposition of particular $1/f$ and generation-recombination (G-R) processes which originate from adsorption and desorption of various atoms present with some residual gas in the vacuum chamber.

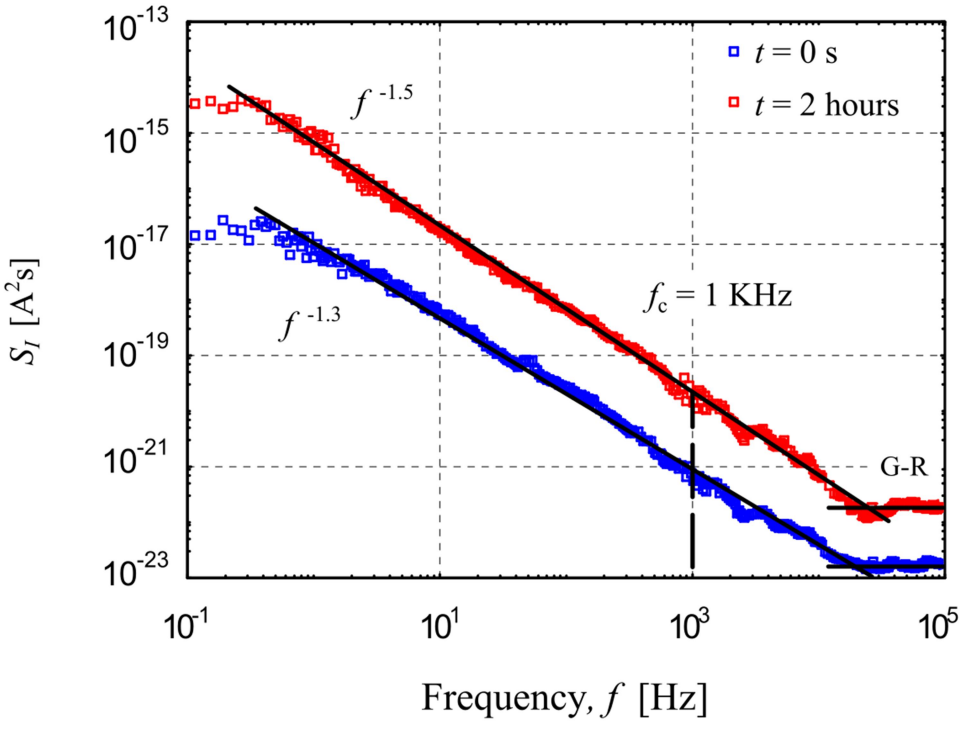

FIG. 9. A comparison of long-time noise power spectrum density measured at $V_{ex} = 200$ V, from $t = 0$s (blue) to $t = 120$ min (red).

The results suggest that the ions which are bombarding the cathode's surface can be observed from the noise measurement as well. They prove themselves by random *burst noise*. The bombardment reduces the epoxy layer, which leads to its unavoidable damage. The noise spectral density (where the $1/f$ noise prevails) changes to $1/f^{n}$, where n is located between 1 and 2. In general, the $1/f^{n}$ noise originates from the superposition of particular $1/f$ and generation-recombination (G-R) processes. Therefore, the higher the n, the more significant

the G-R. Generation-recombination is caused mostly by the chemisorption of the ion residuals present in the chamber. These effects of chemisorption are unavoidable, since only the surface on the tip is protected by the epoxy layer.

Conclusions

In this paper, two similar studies have been compared with the emphasis on similar features, confirming the excellent field emission behavior of the dielectric-coated emitter tip. This is a prospective candidate for a future advanced electron field emitter.

Amongst the most suitable attributes, the most interesting are the low operating voltages and the high current densities. The resin coating protects the surface of the emission plane from unwanted chemical or physical sorption of ions which are attracted backwards towards the cathode and cause a massive bombardment of the tip. This protection enables the cathode to work at lower vacuum than for classical field emission. The coating also slightly reduces the emission current, making the energy more symmetrically distributed compared to the distribution of the uncoated emitter. The epoxy influence of the coating thickness on emission stability will be discussed later in a follow-up publication. For now, it can be concluded that the coating is very thin. Epoxy coating also causes a decrease in the beam energy spectrum which is lower by ≈ 0.7 eV with respect to the Fermi level of the metallic cathode, as we can see in the electron spectra.

Acknowledgements

From the Czech part: The research was supported by the Ministry of Industry and Trade of the Czech Republic, MPO-TRIO project FV10618. The research infrastructure was funded by the Czech Academy of Sciences (project RVO:68081731).

References

[1] Mousa, M.S. and Latham, R.V., Le Journal de Physique Colloques, 47 (C7) (1986) C7-139.

[2] Knápek, A. and Grmela, L., "Methods of Preparation and Characterisation of Experimental Field-Emission Cathodes", (Brno University of Technology, Brno, Czech Republic, 2013).

[3] Knápek, A. and Grmela, L., Chemické Listy, 107 (7) (2013) 545.

[4] Knápek, A. et al., Microelectronic Engineering, 173 (2017) 42.

[5] Mousa, M.S., Karpowicz, A. and Surma, S., Vacuum, 45 (2-3) (1994) 249.

[6] Al-Qudah, A.A., Mousa, M.S. and Fischer, A., IOP Conference Series: Materials Science and Engineering, 92 (2015) 012021.

[7] Mousa, M.S., Surface Science, 231 (1-2) (1990) 142.

[8] Mousa, M.S., Surface and Interface Analysis, 39 (2-3) (2007) 102.

[9] Latham, R.V. and Salim, M.A., Journal of Physics E: Scientific Instruments, 20 (2) (1987) 181.

[10] Knápek, A. et al., Metrology and Measurement Systems, 19 (2) (2012) 417.

[11] Forbes, R.G. et al., Journal of Vacuum Science & Technology B: Microelectronics and Nanometer Structures Processing, Measurement and Phenomena, 22 (3) (2004) 1222.

[12] Mousa, M.S., Le Journal de Physique Colloques, 48 (C6) (1987) C6-115.